Medical Image Fusion with a Shift-Invariant Morphological Wavelet

Bo Yang

College of Information and Electrical Engineering
Shandong University of Science and Technology
Qingdao, China
yangbo.sd@gmail.com

Zhongliang Jing

Institute of Aerospace Science and Technology
Shanghai Jiaotong University
Shanghai, China
zljing@sjtu.edu.cn

Abstract—**This paper presents a novel algorithm for medical image fusion, using a shift-invariant multiscale decomposition scheme. The decomposition scheme is obtained by discarding the downsampling operators of a morphological wavelet. An experiment based on real medical images shows that the proposed method improves the quality of the fused image significantly.**

Keywords—**image fusion, nonlinear wavelet, shift-invariant, medical imaging**

I. INTRODUCTION

Medical image fusion intelligently combines multi-modality medical images for the purpose of providing a more accurate and comprehensive view of a part of the human body. Medical images from different modalities are often significantly complementary. For example, Computerized Tomography (CT) provides the best information on denser tissue, while Magnetic Resonance Imaging (MRI) provides better information on soft tissue. The complementary information existing in medical images provides the possibility for fusion. With the development of medical imaging technology, more and more multi-modality medical images are available in clinical application; the idea of meaningfully combining these images becomes very important and medical image fusion has emerged as a new and promising research field.

Many techniques and schemes for image fusion have been proposed, from the simplest weighted averaging to more advanced pyramidal methods [1]-[3]. Recently, with the development of wavelet technique, it has become popular to use wavelet decomposition in image fusion [4]-[6]. Wavelet is originally known as a linear signal analysis tool, however, more recently, it has been increasingly recognized that nonlinear extensions of wavelet are possible. In [7], Heijmans and Goutsias studied nonlinear wavelets systematically and introduced a series of nonlinear schemes based on mathematical morphology. Nonlinear wavelets with some attractive properties (for details, see [7]) provide new tools for various fusion tasks. In [8], De and Chanda introduced a morphological wavelet for multifocus image fusion.

This paper presents a novel method for medical image fusion, using a shift-invariant morphological wavelet for the decomposition of source images. The proposed method is tested using a pair of CT and MRI images, and the result demonstrates its effectiveness.

II. MORPHOLOGICAL HAAR WAVELET

The Morphological Haar Wavelet (MHW) [7] is the nonlinear extension of the classical Haar Wavelet (HW). The linear filters of the latter are replaced by morphological operators: *dilation* and *erosion* [9]. Let $c_0^{(0)}$ be a input signal, $c_0^{(i)}$ and $c_1^{(i)}$ denote scaling function and wavelet coefficients at level i, respectively. The MHW decomposition can be described as:

$$c_0^{(i)}(n) = c_0^{(i-1)}(2n) \vee c_0^{(i-1)}(2n+1) \qquad (1)$$

$$c_1^{(i)}(n) = c_0^{(i-1)}(2n) - c_0^{(i-1)}(2n+1) \qquad (2)$$

where the dilation operator "$\vee$" means taking the maximum over two samples. Correspondingly, the MHW reconstruction can be written as:

$$r_0^{(i)}(2n) = r_0^{(i)}(2n+1) = c_0^{(i)}(n) \qquad (3)$$

$$r_1^{(i)}(2n) = c_1^{(i)}(n) \wedge 0; \quad r_1^{(i)}(2n+1) = -c_1^{(i)}(n) \vee 0 \qquad (4)$$

which the erosion operator "$\wedge$" means taking the minimum over two samples, $r_0^{(i)}$ and $r_1^{(i)}$ are reconstructed components corresponding to $c_0^{(i)}$ and $c_1^{(i)}$, respectively. The sum of two components reconstructs scaling function coefficients at the previous level:

$$c_0^{(i-1)}(n) = r_0^{(i)}(n) + r_1^{(i)}(n) \qquad (5)$$

III. SHIFT-INVARIANT EXTENSION OF MHW

As compared with general linear wavelets, the MHW has advantages in terms of computation, hardware implementation, and extremum extraction [8]. However, the MHW is not *shift-invariant* [6], [10], [11], the same as the (linear) HW, due to downsampling operations in its standard implementation. Following Kingsbury [10] to illustrate the extent of shift invariance, we compute the projections of a disk image in the wavelet and the scaling function subbands. Fig. 1 (a) shows the

result obtained using the MHW. The projections are severely distorted. The lack of shift invariance will result in severe blocking artifacts in fused images as will be demonstrated in section 5. In this section, we improve the MHW by discarding its downsampling operations and obtain an Undecimated MHW (UMHW), which is shift-invariant. As shown in Fig. 1 (b), perfect arcs are achieved by the UMHW.
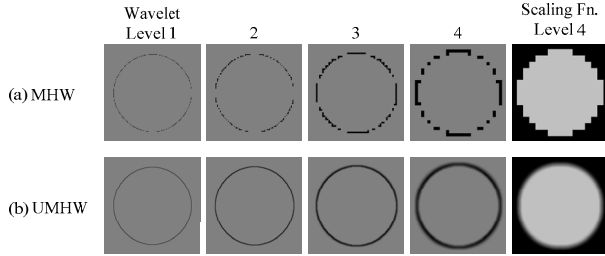

Figure 1.   Shift invariance for the MHW versus the UMHW.

We first extend the noble identity [12] to the morphological case. A morphological operator $S(k)$ is defined in Fig. 2 (a). Downsampling by M before $S(k)$ is equivalent to filtering by $S(Mk)$ and followed by the downsampler, as shown in Fig. 2 (b). Then, using the identity, we derive the equivalent form of the MHW decomposition in the scaling function branch, as shown in Fig. 2 (c), where $c'_0{}^{(i)}$ is the undecimated version of $c_0{}^{(i)}$, i.e.,

$$c_0^{(i)}(n) = [c_0'^{(i)}(n)]_{\downarrow 2^i} = c_0'^{(i)}(2^i n) \qquad (6)$$

Therefore, the scaling function coefficients for the UMHW can be calculated by:

$$c_0'^{(i)}(n) = c_0'^{(i-1)}(n) \vee c_0'^{(i-1)}(n+2^{i-1}) \qquad (7)$$

with $c'_0{}^{(0)} = c_0{}^{(0)}$ (input signal); the wavelet coefficients can be obtained by:

$$c_1'^{(i)}(n) = c_0'^{(i-1)}(n) - c_0'^{(i-1)}(n+2^i) \qquad (8)$$

Correspondingly, the reconstruction equations are extended as:

$$r_0'^{(i)}(n) = \frac{1}{2}[c_0'^{(i)}(n) + c_0'^{(i)}(n-2^{i-1})] \qquad (9)$$

$$r_1'^{(i)}(n) = \frac{1}{2}[c_1'^{(i)} \wedge 0 - c_1'^{(i)}(n-2^{i-1}) \vee 0] \qquad (10)$$

where $r'_0{}^{(i)}$ and $r'_1{}^{(i)}$ are the undecimated version of reconstructed components. Similarly, the sum of two components reconstructs the scaling function coefficients at the previous level, i.e.,

$$c_0'^{(i-1)}(n) = r_0'^{(i)}(n) + r_1'^{(i)}(n) \qquad (11)$$

The undecimated version is still perfect constructed.
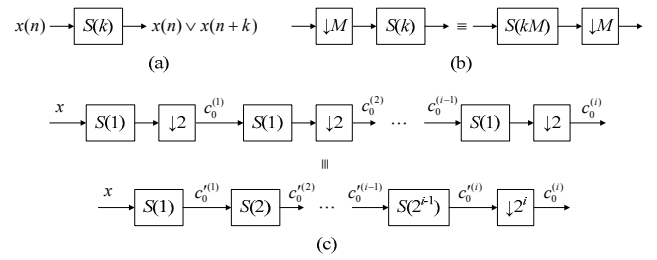

Figure 2.   Derivation of the UMHW: (a) A morphological operator; (b) noble identity for the operator; (c) equivalent transformation for the scaling function branch of the MHW decomposition.

IV.   FUSION SCHEME BASED ON UMHW

As a shift-invariant nonlinear multiscale representation, the UMHW can be applied to advantage in image fusion. To simplify the problem of image fusion, we assume that there are just two source images, A and B; the fused image is F. It should be noted that all the fusion algorithms involved in this work can be easily extended to the cases with more than two source images.

The fusion scheme based on the UMHW, identical with the generic wavelet-based fusion scheme, can be divided into three steps (see Fig. 3). Firstly, both source images are decomposed using the UMHW. Secondly, the coefficient representations of both images are combined into one fused coefficient representation using a fusion rule. Finally, the fused image is obtained by taking the UMHW reconstruction to the fused coefficient representation.
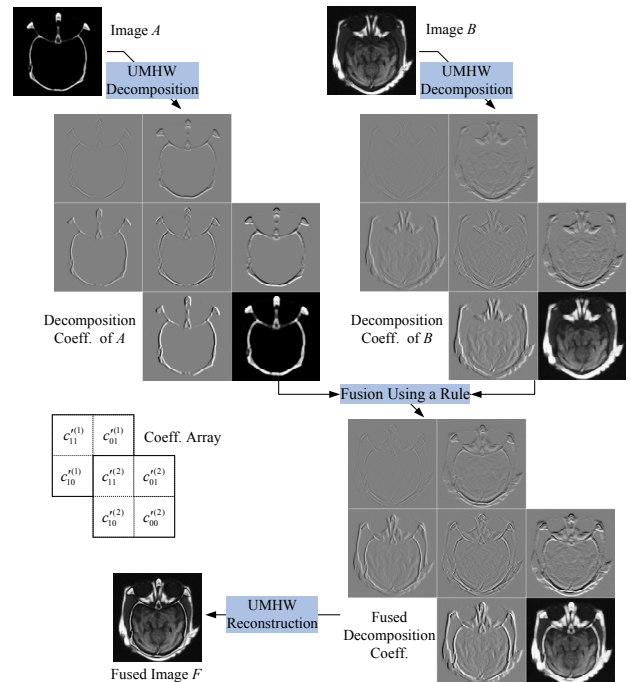

Figure 3.   Illustration of the fusion scheme based on the UMHW

The wavelet coefficients generated by the UMHW depict detail information such as edges or lines in an input image. Absolute value is the simplest activity measurement of these

details. Therefore, the absolute maximum-selection rule is adopted here, i.e.,

$$F\_c_j^{(i)}(m,n) = \begin{cases} A\_c_j^{(i)}(m,n), & \text{if } \left|A\_c_j^{(i)}(m,n)\right| > \left|B\_c_j^{(i)}(m,n)\right|; \\ B\_c_j^{(i)}(m,n), & \text{otherwise.} \end{cases}$$

(12)

where $X\_c_j^{(i)}$ $(j = 01,10,11)$ are the wavelet coefficients of the image X at level i $(i = 1,2,\ldots,I)$. The scaling function coefficients generated by the UMHW are the local maximums of the input image. Larger coefficients correspond to brighter pixels, which normally belong to more important features or regions for medical images and should be preserved as far as possible in the fused image. Based on this observation, the scaling function coefficients are combined by using the maximum-selection rule, i.e.,

$$F\_c_{00}^{(I)}(m,n) = A\_c_{00}^{(I)}(m,n) \vee B\_c_{00}^{(I)}(m,n) \qquad (13)$$

where $X\_c_{00}^{(I)}$ is the scaling function coefficients of the image X at the last level.

The UMHW scheme adopts 2-level decomposition, less than linear wavelet methods (normally adopt 4-level), due to the good ability of edges preservation for morphological operators [7]. The reduction of decomposition levels enhances the computational advantage of the UMHW method, potentially.

V. RESULTS

The UMHW scheme has been tested on real medical images, and has been compared with these schemes using the HW [4], the Undecimated HW (UHW) [5], and the MHW [7]. Fig. 4 (a) and (b) show a pair of Computer Tomography (CT) and Magnetic Resonance Imaging (MRI) images (obtained from www.imagefusion.org, provided by O. Rockinger). Fig. 4 (c) - (f) show the results fused using various methods. The HW and the MHW schemes result in visible "blocking" artifacts duo to lack of shift-invariance. The undecimated schemes, the UHW and the UMHW schemes, effectively eliminate these artifacts; however, the latter is much better than the former in the visual brightness of fused images.

The Edge Preservation (EP) [13] and the Mutual Information (MI) [14] metrics were computed to assess performance quantitatively. Table 1 indicates that the proposed scheme performs better than other concerned methods in the preservation of both "edge" and "pixel" information.

VI. CONCLUSION

We have presented a shift-invariant morphological wavelet by discarding the downsampling operation of the morphological Haar wavelet. Based on this wavelet, we proposed a shift-invariant scheme for medical image fusion. The scheme is computationally simple and very suitable for hardware implementation, benefiting from the use of morphological operators. Experimental results showed that the proposed scheme is definitely better than the shift-variant schemes based on the Haar wavelet and the morphological

Haar wavelet, as well as better than the linear shift-invariant scheme based on the undecimated Haar wavelet.

| (a) CT | (b) MRI | (c) HW |

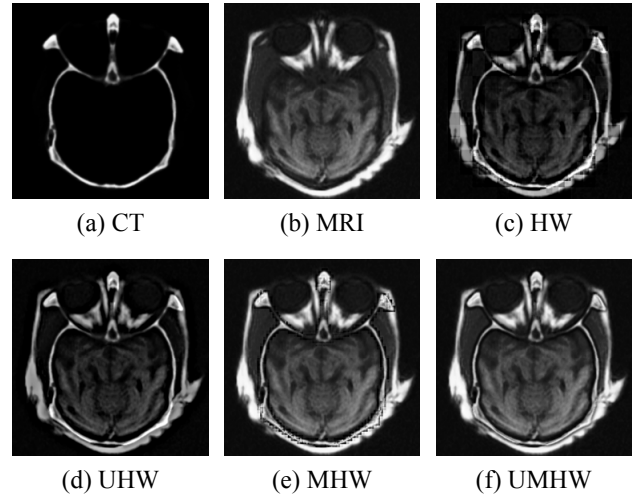| (d) UHW | (e) MHW | (f) UMHW |

Figure 4. Image fusion with medical images: (a) and (b) are source images; (c) - (f) are fused images using HW, UHW, MHW, and UMHW, respectively.

TABLE I. QUANTITATIVE RESULT FOR MEDICAL IMAGE FUSION

Fusion Schemes	EP	MI
HW	0.6544	3.1400
UHW	0.7390	2.9250
MW	0.7497	5.3491
UMHW (the proposed)	0.7851	5.4720

REFERENCES

[1] P.J. Burt, E.H. Adelson, Merging images through pattern decomposition, in: Proc. of SPIE, 1985, vol. 575, pp. 173-181.

[2] A. Toet, L.J. Ruyven, J.M. Valeton, Merging thermal and visual images by a contrast pyramid, Optical Engineering, 28 (1989) 789-792.

[3] P.J. Burt, R.J. Kolczynski, Enhanced image capture through fusion, in: Proc. of Int. Conf. on Computer Vision, Berlin, Germany, 1993, pp. 173-182.

[4] H. Li, B.S. Manjunath, S. Mitra, Multisensor image fusion using the wavelet transform, Graphical Models and Image Process, 57 (1995) 235-245.

[5] O. Rockinger, Image sequence fusion using a shift invariant wavelet transform, in: Proc. of Int. Conf. on Image Process. 1997, vol. 3, pp. 288-291.

[6] B. Yang, Z.L. Jing, Image fusion using a low-redundant and nearly shift-invariant discrete wavelet frame, Optical Engineering, 46 (2007) 107002.

[7] H.J.A.M. Heijmans, J. Goutsias, Nonlinear multiresolution signal decomposition schemes—Part II: Morphological wavelets, IEEE Trans. Image Process. 9 (2000) 1897-1913.

[8] I. De, B. Chanda, A simple and efficient algorithm for multifocus image fusion using morphological wavelets, Signal Processing, 86 (2006) 924-936.

[9] H.J.A.M. Heijmans, Morphological Image Operators, MA: Academic, Boston, 1994.

[10] N.G. Kingsbury, Complex wavelets for shift invariant analysis and filtering of signals, Applied and Computational Harmonic Analysis, 10 (2001) 234-253.

[11] B. Yang, Z.L. Jing, A simple method to build oversampled filter banks and tight frames, IEEE Trans. Image Process. 16 (2007) 2682-2687.

[12] P.P. Vaidyanathan, Multirate digital filters, filter banks, polyphase networks, and applications: a tutorial, Proc. of IEEE, 78 (1990) 56-93.

[13] C.S. Xydeas, V. Petrović, Objective image fusion performance measure, Electronics Letters, 36 (2000) 308-309.

[14] G. Qu, D. Zhang, P. Yan, Information measure for performance of image fusion, Electronics Letters, 38 (2002) 313-315.